Lab on a Chip

Cite this: *Lab Chip*, 2012, **12**, 1897

www.rsc.org/loc

**TECHNICAL NOTE**

# Real time quantitative amplification detection on a microarray: towards high multiplex quantitative PCR

**Anke Pierik,*[a] Marius Boamfa,[a] Martijn van Zelst,[a] Danielle Clout,[a] Henk Stapert,[a] Frits Dijksman,[a] Dirk Broer[b] and Reinhold Wimberger-Friedl[a]**

***Received 10th August 2011, Accepted 24th February 2012***
**DOI: 10.1039/c2lc20740k**

Quantitative real-time polymerase chain reaction (qrtPCR) is widely used as a research and diagnostic tool. Notwithstanding its many powerful features, the method is limited in the degree of multiplexing to about 6 due to spectral overlap of the available fluorophores. A new method is presented that allows quantitative amplification detection at higher multiplexing by the integration of amplification in solution and monitoring *via* hybridization to a microarray in real-time. This method does not require any manipulation of the PCR product and runs in a single closed chamber. Employing labeled primers, one of the main challenges is to measure surface signals against a high fluorescence background from solution. A compact, confocal scanner is employed, based on miniaturized optics from DVD technology and combined with a flat thermocycler for simultaneous scanning and heating. The feasibility of this method is demonstrated in singleplex with an analytical sensitivity comparable to routine qrtPCR.



The method as presented here combines two powerful and well established techniques to achieve a high multiplex quantitative PCR detection *i.e.* quantitative real time PCR (qrtPCR) in solution and hybridization to microarrays. QrtPCR being unmatched in sensitivity is limited in the degree of multiplexing due to the need for distinct optical channels.[1] In order to increase the degree of multiplexing one can split the sample into multiple reaction wells and perform different qrtPCRs in each well. The procedure is straightforward; however, it has the disadvantage of a reduced sensitivity since the sample needs to be divided. Therefore, the lower limit of detection will increase proportional to the number of wells.

Microarrays are commonly used for parallel detection of multiple targets. Capture probes complementary to a specific target sequence are immobilized as spots on the microarray surface. After incubation with the fluorophore-labeled targets, the fluorescence spot intensities are measured, providing information on the presence and the concentration of the targets in the sample. Multiplexing is obtained by spatial separation of the different probes on the microarray surface rather than using different fluorescently labeled probes as in qrtPCR. The disadvantage of this method is that it is not possible to quantify the initial number of target molecules present in the sample before amplification, like in qrtPCR.

By integrating qrtPCR with microarray hybridization detection, high multiplexing can be achieved by spatial probe separation and by the integration into a single chamber process with no post-PCR handling steps to minimize chances of cross-contamination.

Real time hybridization detection of PCR products has been reported in the literature.[2–7] The integration of DNA amplification with detection steps in a single volume has also previously been published, but in those cases only end-point PCR followed by hybridization was performed,[8–10] which does not provide quantitative information. Furthermore, methods have been presented in which quantification is based on stopping the PCR in the logarithmic phase, followed by hybridization to a microarray.[11] These steps were not integrated. The dynamic range of such a method is limited, and does not satisfy the requirements of many applications.[12]

In order to achieve an integrated and quantitative method, measurements need to be performed throughout the amplification process, like in regular qrtPCR.[13] To accomplish this, a number of challenges need to be overcome. The reagent mixture containing PCR products, PCR ingredients and labeled primers is in contact with the microarray. Even when scanning or imaging the fluorescence background through the substrate, a high background signal is observed. Background suppression needs to be achieved. Furthermore, hybridization and detection must be carried out rapidly, ideally within one minute, to not lengthen the total amplification process dramatically. Short hybridization time leads to low coverage of the spots and thus low signals. A challenge of real time array PCR is thus the rapid and sensitive

[a]*Philips Research, High Tech Campus 11, 5656 AE Eindhoven, The Netherlands. E-mail: anke.pierik@philips.com*
[b]*Eindhoven University of Technology, Den Dolech 2, 5612 AZ Eindhoven, The Netherlands*

detection of hybridization on the microarray surface against a high background fluorescence. Additionally, the integration of PCR and hybridization implies that hybridization must be done under low-salt circumstances needed for the PCR, while hybridization is usually performed in high-salt buffers.

Fluorescence detection methods that allow for a substantial background reduction, like evanescent wave excitation based on total internal reflection, have been patented.[14] Instead of using advanced technologies or background suppression, the challenge can also be addressed by designing a method that does not create high background to begin with. In ref. 15 and 16 a real time multiplex PCR method is described that makes use of immobilized primers which are elongated in hydrogel pads on the substrate surface. Detection of hybridized targets to the elongated primers was done by measuring the fluorescence of SYBR green by a (CCD) camera. By use of an intercalating dye, the background level scales with the amplicon concentration. However, the attainable contrast with intercalating dyes is low due to limited specificity.

Multiplexing PCR can be defined in different ways with different implications, *i.e.* multiplexing the primer sequences and/or multiplexing the probe sequences. When using labeled probes in solution, like Taqman, every probe requires a separate spectral range which is very constraining. Using spatially separated probes on a microarray can alleviate this limitation. One can then directly label the amplicons by using covalently labeled primers or secondary labeling, either non-specific (*e.g.* intercalators) or specific (labeled probes). Secondary labeling typically has a lower dynamic range and also lower background levels. Alternatively, labeled immobilized probes can be employed which change emission upon target hybridization (*e.g.* molecular beacons). In that case again the dynamic range is limited by the quenching efficiency but the probe design can be challenging for higher degrees of multiplexing. The use of multiple probes for every primer pair allows multiplexing of homologous templates, like pathogens subtypes, or SNPs. The multiplexing is not only limited by optical constraints but also limited by primer–primer interactions which cannot be overcome by optical detection or labeling strategies.

In our approach we build on proven and robust technology as much as possible. We use labeled primers to have freedom in probe design. As a consequence one needs strong background suppression to deal with the fluorescence generated by the labeled primers in solution. Confocal scanning is a well-known technique in microarrays with a high signal to noise ratio. Confocal detection not only suppresses fluorescence outside the focal volume of the optical beam but also eliminates contributions of auto-fluorescence of the optical components in the light path. At the same time the luminescence of the spots is enhanced by the high excitation intensity of a focused beam and the collected efficiency of the objective lens with a high numerical aperture. Using an epi-fluorescence arrangement the heater can be provided at the opposite side of the scanning optics.

Leveraging Philips' know-how in optical storage technology, a very compact fluorescence scanner was developed with an integrated thermocycler. The scanner is equipped with an auto-focus mechanism. The objective lens (NA = 0.65) is compensated for the substrate thickness, yielding a diffraction-limited spot (HWFM 0.6 micron, 660 nm wavelength) on the substrate surface facing the PCR chamber. Scanning is accomplished by moving the objective with an x,y-stage driven by low-cost linear motors. The cartridge is not moved. Fig. 1a–d depicts the cartridge, the integrated instrument, the thermocycler, and a schematic cross-section with the light beam, respectively. The set-up can also be used for real-time hybridization and melting curve analyses.

Due to the use of miniaturized off-the-shelf components, the instrument is compact and has low cost-of-goods.

Amplification is performed in a three-step PCR with both primers in solution, one of which is labeled. During the annealing phase, hybridization of the labeled amplicons to the complementary probes on the microarray takes place. By monitoring fluorescence at the end of the annealing phase of every cycle, an S-shaped curve is obtained, resembling a traditional qrtPCR curve from which the cycle threshold value (Ct-value) can be determined and used for quantification of the input. Since hybridization/annealing times are limited to only a few minutes, the fraction of occupied capture probes on the spots is relatively low. As a result, effects like fluorescence quenching, surface crowding and dissociation of the bound labeled amplicons back into the solution do not play a role. Taking these aspects into account, it is reasonable to assume that the fluorescence measured on the microarray spot scales linearly with the concentration of amplicons in solution. Towards the end of the amplification process where the concentration of labeled amplicons is much higher (typically tens of nanomolar concentration), this assumption might not be valid anymore. However, since the Ct-value, which is obtained at low amplicon concentrations, is used for quantification, this will not affect the result of the qrtPCR.

As a model system the *femA* gene of the methicillin-sensitive *Staphylococcus epidermidis* (MSSE) genome was used. To investigate the amplification characteristics, 250 000 copies of this gene were amplified using both conventional qrtPCR and real time array PCR. Standard commercial Master Mix was mixed with template and primers and then injected into a PCR chamber *via* a standard syringe connector (see Fig. 1a).

In Fig. 2a amplification curves are depicted as obtained during amplification with both methods (dashed line, conventional qrtPCR; solid line, real time array PCR). For comparison, the fluorescence intensities are normalized to the maximum value of each measurement. As can be seen, the two PCR curves are similar, though the steepness of the real time array PCR curve is lower, which might be attributed to a reduced amplification efficiency in the bulk. The Ct-values of both methods are comparable. A four-parameter Boltzmann curve fit which is a common method for PCR curve fitting[17] was used to fit the rt-array-PCR curve (fit quality $R^2 = 0.98$). In Fig. 2b, the microarray images are shown for the 1$^{st}$, 40$^{th}$ and 60$^{th}$ cycle, respectively. As can be seen, the hybridization spots do not show a signal after the 1$^{st}$ cycle, but have increasing fluorescence at cycles 40 and 60. The negative control spots show no hybridization signals, as expected. For details, see the figure caption.

A dilution series from 250 000 to 25 molecules per reaction of the MSSE genome was performed. Fig. 3 presents the Ct-values *versus* input copy numbers for qrtPCR and real time array PCR. The lowest copy number could still be detected using real time array PCR, whereas no template control (NTC) was negative as expected. From these data, a semi-log fit between input concentration and Ct-value was obtained, which was used to evaluate the PCR efficiency. An efficiency of 97% was found in

 

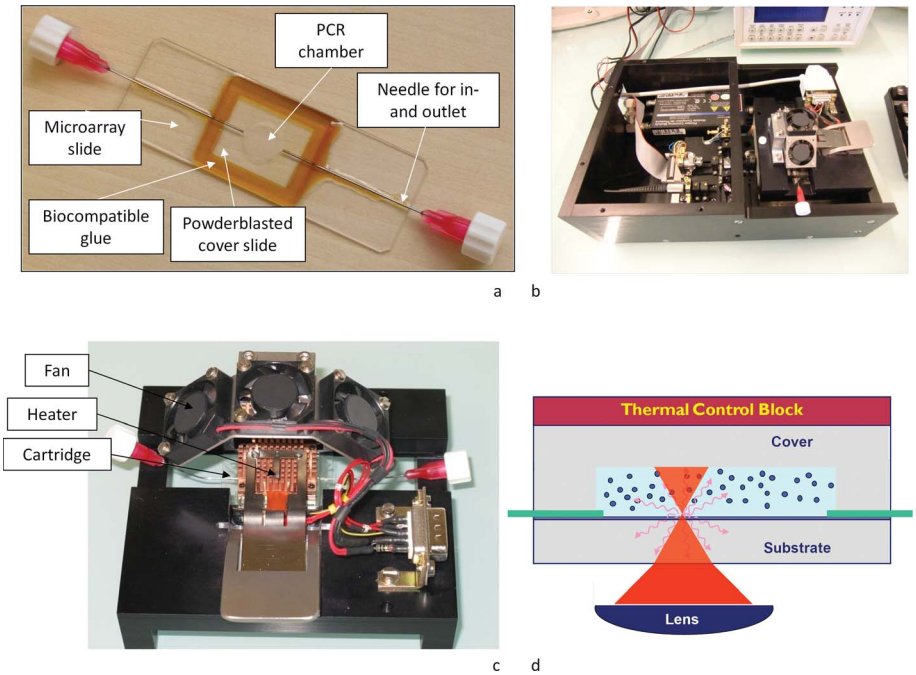


**Fig. 1** Cartridge (a) and instrument (b) prototype of the complete integrated fluorescent scanner (c) thermocycler set-up for real time array PCR, and the schematic cross-section (d).

qrtPCR, whereas the array PCR efficiency was 58%. For the higher target input concentrations, similar Ct-values were found between qrtPCR and real time array PCR even with a reduced amplification efficiency compared to qrtPCR. This means that intrinsically the detection sensitivity is at least as good as qrtPCR.[18]

There are a few possible explanations for the lower efficiency of real time array PCR. A first consideration is that amplicons

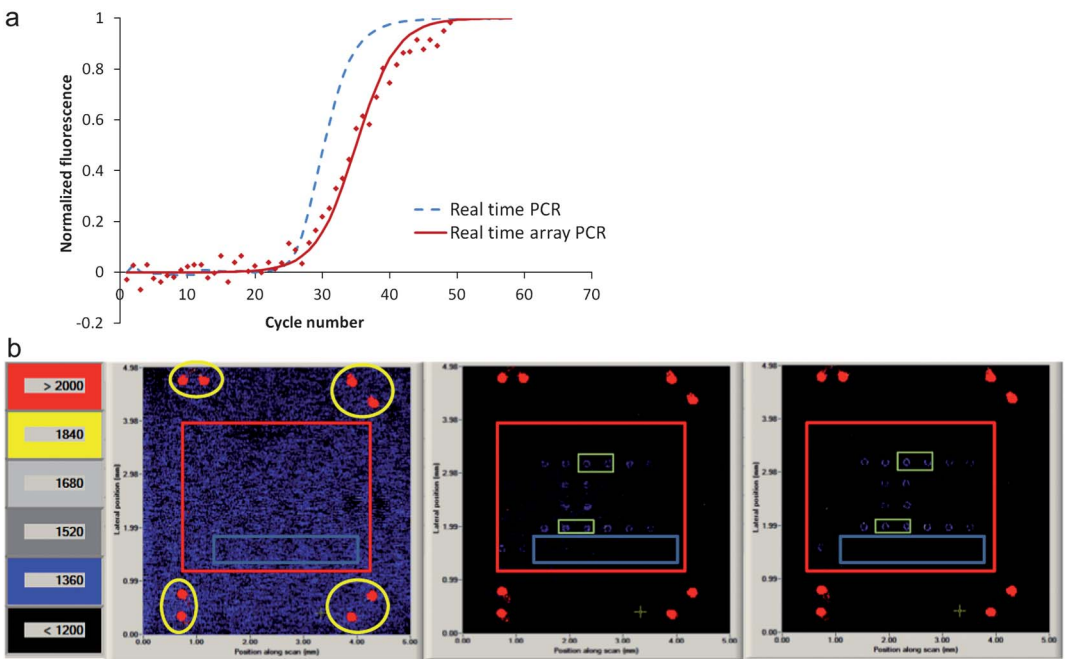


**Fig. 2** (a) The amplification curves of 250 000 copies input target molecules of the *femA* gene of the *S. epidermidis* genome, as recorded in conventional qrtPCR (blue dashed line) and with real time array PCR (the red diamond markers are the raw data points, the red solid line represents the curve fit). The fluorescence intensities are normalized to the maximum value of each measurement for convenience of comparison. (b) A scan of the microarray after 1 (left), 40 (middle) and 60 (right) cycles. The yellow circles depict the fluorescent spots used for alignment of the microarray. The blue rectangle visualizes the negative control spots (oligonucleotides having no homology to the target sequence). The spots in the red rectangle (except for the spots in the blue rectangle) mark the hybridization spots. Included are different sequences homologous to the target sequence (data not shown), which were used for optimization. Only the spots in the green rectangle were used for the analysis.

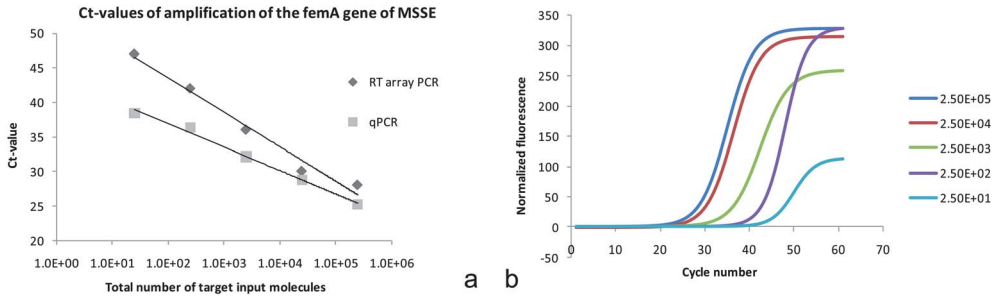


**Fig. 3** (a) Cycle threshold values for qrtPCR and real time array PCR *vs.* target input and (b) fits of background corrected real time array PCR curves for different target inputs as indicated. The $R^2$ values for the linear trend lines in the left graph are 0.99 for the qrtPCR and 0.98 for the real time array PCR results, respectively.

hybridized to the probes on the microarray surface might not be available for elongation. The fraction of amplicons that can diffuse towards the microarray surface during the annealing phase of each PCR cycle was calculated as less than 0.1%. Therefore this effect cannot explain the reduced amplification efficiency. This was also confirmed by qrtPCR experiments (data not shown), in which capture probes were added to the solution without any noticeable difference in results.

A second consideration is loss of polymerase activity due to either non-specific adsorption to the cartridge surfaces or thermal degradation. Non-specific protein adsorption followed by protein denaturation to glass or related materials is a well-known phenomenon. Non-specific enzyme adsorption to the cartridge walls can thus be a source of the reduced PCR efficiency.[19] Bovine serum albumin (BSA) is a known blocking agent that prevents other proteins from adsorbing onto the surface.[19,20] A strong positive effect of adding BSA was confirmed by experiment: by excluding BSA in the reaction mix, no PCR curves where obtained at all. Regarding the effect of thermal degradation, enzymes are known to be extremely sensitive to thermal degradation[21] at temperatures exceeding 95 °C. Thermal degradation could lead to a lack of available enzyme which can become critical particularly at high cycle numbers. As a result Ct-values of amplification reactions using low target input numbers will be affected most. In fact, the heater settings in the thermocycler were offset by 3 °C to compensate for gradients due to heat transfer to the cartridge. As a consequence, the temperature could reach values higher than 95 °C locally during the denaturing phase. Preliminary experiments with higher enzyme concentrations have shown improved results (data not shown). Further improvement of the thermal control of the cartridge is expected to increase efficiency.

The overall time to create a full array PCR curve was around 3.5 h for 60 cycles. This is longer than that for a standard 2-step qrtPCR protocol that can perform 60 cycles in less than 2 h. So far heating and cooling rates have not been optimized in the prototype system. The main intrinsic difference between the two methods lies in hybridization kinetics. In qrtPCR, hybridization occurs in the bulk. The binding rate can be increased by employing high probe concentrations. In array-PCR, the probes are bound to the surface which is equivalent to a low concentration, so probe hybridization will be slower. The achievable speed is determined by the detection sensitivity of the instrument. The scanning time does not add significantly to the total cycle time for reasonable array dimensions ($\leq$1 cm$^2$).

So far only singleplex model systems have been used for investigating the potential of our method. Therefore, one of the focus points for future work is the implementation of multiplex assays. Multiplexing can be done as in qrtPCR systems and thus the degree of multiplexing can be limited by the number of PCRs itself. The most promising application area is in the detection of many highly homologous target sequences which can be amplified with a limited number of primer pairs, like pathogen resistance testing, viral (*e.g.* HPV, HCV, HIV) genotyping or SNP detection (*e.g.* cystic fibrosis).

In conclusion, proof of concept has been shown of monitoring PCR amplification on a microarray by confocal scanning using a cost-effective instrument and standard qrtPCR reagents. This method enables increased multiplexing of qrtPCR with comparable detection sensitivity as qrtPCR. Since amplification and detection are carried out in a single, closed cavity thereby minimizing lab contamination, it is particularly suited for decentralized diagnostic testing. The compact and low-cost approach even enables point-of-care applications of this new method.

## Methods

### Microarray fabrication

All capture probes (Biolegio, Nijmegen, The Netherlands) were dissolved to concentrations of 3 μM in a 75 mM sodium phosphate buffer of pH 8.5 (all ingredients from Sigma-Aldrich, St-Louis, MO, USA). Superamine2 microarray glass slides (ArrayIt Corporation, Sunnyvale, CA, USA) were used. Each capture probe solution was deposited by an in-house developed inkjet printer[22] in four-fold onto the substrates using 1 nanolitre total spot volume. Before printing, the droplet volume is measured and the number of droplets needed for the 1 nanolitre spot volume is automatically calculated, thereby reducing variations in surface density of the spot to around ±10%. Spot signals are likely to be proportional to the surface density of the probes in the spots. However, variations in this order of magnitude will not impact the quantification process due to the exponential behavior of real time array PCR. The resulting spot diameters were app. 200 μm.

All capture probes were 5′-end modified with 16 thymines for optimal immobilization during the subsequent photo-activated cross-linking step[23] by exposure to 300 mJ cm$^{-2}$ of 254 nm UV light. This was followed by a combined washing and blocking step for 1 h at 42 °C in 5× SSC, 0.1% SDS and 0.1 mg ml$^{-1}$

 

herring sperm DNA (all ingredients from Sigma-Aldrich, St-Louis, MO, USA).

Negative control spots were included for investigation of the specificity of the hybridization. This was done by spotting an oligonucleotide onto the microarray having a sequence with no homology to the target template.

Fluorescently labeled oligo-nucleotide spots also having no sequence homology to the target templates were used for alignment of the microarray with the scanning optics.

Onto the printed microarray slide, a cover glass with a powder-blasted cavity was glued (Epotek 353ND from Epoxy Technologies). A reaction chamber of 25 µl volume was created by the sandblasted cavity and the substrate. This cavity was connected to two syringe dispenser tips (5125-1.5-B type from EFD) for inlets and outlets (prior to epoxy application the needles were fixed with Dymax 142-M (5), biocompatible UV-curable adhesive).

### Real time array PCR system

The experimental system combines confocal fluorescence detection with thermal cycling in a compact device. The scanner is built around a standard DVD pick-up unit (objective lens NA = 0.65) with an auto-focus feedback loop, locked to the microarray surface inside the chamber. The bi-aspheric lens is corrected for the substrate thickness. A diffraction-limited spot (HWFM 0.6 µm, $\lambda$ 660 nm) is scanned over the microarray surface at typically 50 mm $s^{-1}$. An image is created by a meander-like movement driven by an x,y-stage with motors from the tray of a DVD player. The forward resolution is determined by the integration time, the lateral step size can be chosen (min. 1 µm). For the array-PCR experiment scans were built out of 200 lines, 5 mm long, and taken at a lateral step of 25 µm to cover the 5 × 4 mm area of the microarray in about 40 s. The sample holder includes a thermal unit with clamps that hold the cartridge tightly in place to ensure good thermal contact. The heating is achieved by a commercial thin film heater and cooling by means of three fans from a PC motherboard. The temperature of the heater surface is actively controlled in closed loop (PID).

### Real time array PCR

All PCR ingredients and the target template were mixed and diluted into 1× Geneamp Fast PCR Master mix (Applied Biosystems, CA, USA). 0.1% BSA was added for reducing non-specific binding. An optimum of 0.1 w/v% BSA was used during a preceding optimization study (data not shown), since higher concentrations of BSA are known to inhibit the PCR.[19] As a model system the *femA* gene of methicillin-susceptible *S. epidermidis* was used;[17] the amplicon length is 172 basepairs. Both the forward and reverse primers were applied in 300 nM final concentration, see Table 1. All reverse primers were 5′-end Cyanine-5 (Cy5) labeled (Biolegio, Nijmegen, The Netherlands). The target input ranged from 25 to 250 000 copies per amplification reaction.

The PCR program started with a 10 min hot start at 95 °C, followed by 60 cycles of each 40 s at 75 °C, 20 s at 98 °C and 120 s at 55 °C. During the last 40 s of the annealing phase, hybridization signals were measured. Capture probes that were 40 nucleotides in length were designed based on the Taqman sequences as found in the literature.[24] Slightly longer capture probes compared to the Taqman sequences were used for improved hybridization kinetics as found in an earlier optimization study, see Table 1.

### Fluorescence measurements and calculations

The fluorescence intensities of all spots present on the microarray are measured at the end of the annealing step. For each hybridization measurement, the average fluorescent intensity of two spots of the same capture probe sequence were used. Background correction was done by subtracting average background fluorescence in the vicinity of the spots. Ct-values were calculated by determining the cycle number at which the (background corrected) fluorescence intensity exceeded three times the average standard deviation on the background (background is taken as the fluorescence of cycles 1–15).

### Conventional qrtPCR

For reference, quantitative real-time PCR (qrtPCR) experiments were performed on a Bio-rad CFX96 system (Hercules, CA, USA). For detection, a Taqman probe was used, see Table 1, with a sequence identical, but shorter, to the capture probe used for the real time array PCR, since a shorter sequence turned out to be more effective for qrtPCR. This probe also contained a tail of 16 thymines, which did not influence the amplification (data not shown).

The qrtPCR protocol was optimized for having the fairest benchmark, which was after an initial hot-start 60 cycles of 15 s at 95 °C followed by 60 s at 60 °C. The same Master Mix was used.

**Table 1** The oligonucleotides and their corresponding sequences are used in this study.

| Oligonucleotide type | Oligonucleotide sequence |
|---|---|
| *femA* SE forward primer | 5′-CAA CTC GAT GCA AAT CAG CAA-3′ |
| *femA* SE reverse primer | 5′-GAA CCG CAT AGC TCC CTG C-3′ |
| *femA* SE capture probe | 5′-AAG TAG TTT ACT ACG CTG GTG GAA CTT CAA ATC GTT ATC G-3′ |
| *femA* SE Taqman probe | 5′-TAC TAC GCT GGT GGA CTT CAA ATC GTT ATC G-3′ |
| *femA* SE amplicon | 5′-CAA CTC GAT GCA AAT CAG CAA AAA ATT AAT GAA GCT AAA AAC TTA AAA CAA GAA CAT GGC AAT GAA TTA CCC ATC TCT GCT GGC TTC TTT ATA ATT AAT CCG TTT GAA GTA GTT TAC TAC GCT GGT GGA ACT TCA AAT CGT TAT CGC CAT TTT GCA GGG AGC TAT GCG GTT C-3′ |

## Acknowledgements

The authors would like to thank Faustin Usabuwera and Jan van Beek (both Philips Innovation Services) for printing the microarrays and making the cartridges, respectively.

## References

1 J. A. M. Vet, A. R. Majithia, S. A. E. Marras, A. Tyagi, S. Dube, B. J. Poiesz and F. R. Kramer, *Proc. Natl. Acad. Sci. U. S. A.*, 1999, **96**, 6394–6399.
2 A. L. Ghindilis, M. W. Smith, K. R. Schwarzkopf, C. Zhan, D. R. Evans, A. M. Baptista and H. M. Simon, *Electroanalysis*, 2009, **21**, 1459–1468.
3 A. Pierik, C. Zwanenburg, E. Moerland, D. Broer, H. Stapert and A. van den Brule, *J. Clin. Microbiol.*, 2011, **49**, 1395–1402.
4 H. Dai, M. Meyer, S. Stepaniants, M. Ziman and R. Stroughton, *Nucleic Acids Res.*, 2002, **30**, e86.
5 D. I. Stimpson, J. V. Hoijer, W. Hsieh, C. Jou, J. Gordon, T. Theriault, R. Gamble and J. D. Baldeschwieler, *Proc. Natl. Acad. Sci. U. S. A.*, 1995, **92**, 6379–6383.
6 Y. Wu, P. de Kievit, L. Vahlkamp, D. Pijnenburg, M. Smit, M. Dankers, D. Melchers, M. Stax, P. J. Boender, C. Ingham, N. Bastiaensen, R. de Wijn, D. van Alewijk, H. van Damme, A. K. Raap, A. B. Chan and R. van Beuningen, *Nucleic Acids Res.*, 2004, **32**, e123.
7 W. Michel, T. Mai, T. Naiser and A. Ott, *Biophys. J.*, 2007, **92**, 999–1004.
8 M. Von Nickisch-Rosenegk, X. Marschan, D. Andresen, A. Abraham, C. Heise and F. F. Bier, *Biosens. Bioelectron.*, 2005, **20**, 1491–1498.
9 D. Andresen, M. von Nickisch-Rosenegk and F. F. Bier, *Clin. Chim. Acta*, 2009, **403**, 244–248.
10 D. Trau, T. M. H. Lee, A. I. K. Lao, R. Lenigk, I.-M. Hsing, N. Y. Ip, M. C. Carles and N. J. Sucher, *Anal. Chem.*, 2002, **74**, 3168–3173.
11 S. C. Donhauser, D. Niessner and M. Seidel, *Anal. Chem.*, 2011, **83**, 3153–3160.
12 A. Hassibi, H. M. Vikalo, J. L. Riechmann and B. Hassibi, *Nucleic Acids Res.*, 2009, **37**, e132.
13 S. Yang and R. E. Rothman, *Lancet Infect. Dis.*, 2004, **4**, 337–348.
14 Eppendorf Array Technologies, *WO pat.*, appl. WO2006053770, 2006.
15 D. A. Khodakov, N. V. Zakharova, D. A. Gryadunov, F. P. Filato, A. S. Zasedatelev and V. M. Mikhailovich, *BioTechniques*, 2008, **44**, 241–248.
16 B. N. Strizhkov, A. L. Drobyshev, V. M. Mikhailovich and A. D. Mirzabekov, *BioTechniques*, 2000, **29**, 844–857.
17 A.-N. Spiess, C. Feig and C. Ritz, *BMC Bioinformatics*, 2008, **9**, 221.
18 L. Novak, P. Neuzil, J. Pipper, Y. Zhang and L. Shinhan, *Lab Chip*, 2007, **7**, 27–29.
19 I. Erill, S. Campoy, N. Erill, J. Barbé and J. Aguiló, *Sens. Actuators, B*, 2003, **96**, 685–692.
20 D. S. Shin, K. N. Lee, K. H. Jang, J. K. Kim, W. J. Chung, Y. K. Kim and Y. S. Lee, *Biosens. Bioelectron.*, 2003, **19**, 485–494.
21 J. Sambrook and D. W. Russell, in *Molecular Cloning*, Cold Spring Harbor Laboratory Press, 3rd edn, 2001.
22 A. Pierik, J. F. Dijksman, A. T. A. Raaijmakers, A. J. J. Wismans and H. R. Stapert, *Biotechnol. J.*, 2008, **3**, 1581–1590.
23 A. Pierik, J. F. Dijksman, J. Lub, H. R. Stapert and D. J. Broer, *Anal. Chem.*, 2010, **82**, 1191–1199.
24 P. Francois, D. Pittet, M. Bento, B. Pepey, P. Vaudaux, D. Lew and J. Schrenzel, *J. Clin. Microbiol.*, 2003, **41**, 254–260.



 